Journal of Power Sources 183 (2008) 295–302

Contents lists available at ScienceDirect

Journal of Power Sources

journal homepage: www.elsevier.com/locate/jpowsour

Simulation of a fuel reforming system based on catalytic partial oxidation

Keith L. Hohn[a,*], Terry DuBois[b]

[a] 1005 Durland Hall, Department of Chemical Engineering, Kansas State University, Manhattan, KS 66506-5102, United States
[b] U.S. Army Communications – Electronic Command, Research, Development and Engineering Center, 10125 Gratoit Road, Suite 100, Fort Belvoir, VA 22060-5816, United States

ARTICLE INFO

Article history:
Received 4 January 2008
Received in revised form 2 April 2008
Accepted 4 April 2008
Available online 22 April 2008

Keywords:
Catalytic partial oxidation
Hydrogen
Fuel reforming
JP-8

ABSTRACT

Catalytic partial oxidation (CPO) has potential for producing hydrogen that can be fed to a fuel cell for portable power generation. In order to be used for this purpose, catalytic partial oxidation must be combined with other processes, such as water-gas shift and preferential oxidation, to produce hydrogen with minimal carbon monoxide. This paper evaluates the use of catalytic partial oxidation in an integrated system for conversion of a military logistic fuel, JP-8, to high-purity hydrogen. A fuel processing system using CPO as the first processing step is simulated to understand the trade-offs involved in using CPO. The effects of water flow rate, CPO reactor temperature, carbon to oxygen ratio in the CPO reactor, temperature of preferential oxidation, oxygen to carbon ratio in the preferential oxidation reactor, and temperature for the water-gas shift reaction are evaluated. The possibility of recycling water from the fuel cell for use in fuel processing is evaluated. Finally, heat integration options are explored. A process efficiency, defined as the ratio of the lower heating value of hydrogen to that of JP-8, of around 53% is possible with a carbon to oxygen ratio of 0.7. Higher efficiencies are possible (up to 71%) when higher C/O ratios are used, provided that olefin production can be minimized in the CPO reactor.

1. Introduction

Polymer electrolyte membrane fuel cells (PEMFCs) offer significant potential as portable power sources. In particular, the United States military is considering them as replacements for batteries, since battery power density and lifetime are often not ideal. PEMFCs operate by reacting hydrogen and oxygen to generate electricity. However, hydrogen is difficult to store and transport, so PEMFCs are likely to be powered by liquid fuels, where the liquid fuels are first converted to hydrogen before being fed to the fuel cell.

Converting liquid fuels to high-purity hydrogen is a significant technical challenge, as discussed by a number of authors [1–6]. Sulfur must first be removed from the fuel, since the noble metal catalysts used in the conversion process are susceptible to deactivation by sulfur. Next, the fuel must be reformed to make hydrogen. This reforming step can be achieved by steam reforming, autothermal reforming, or catalytic partial oxidation [7]. The reformed stream contains a high concentration of carbon monoxide, which must be removed before feeding to the fuel cell. A first step to accomplish this is the water-gas shift reaction, which reacts carbon monoxide and water to make carbon dioxide and hydrogen. The carbon monoxide concentration is still too high following this reaction, so selective oxidation is next used to oxidize carbon monoxide to carbon dioxide.

Catalytic partial oxidation (CPO) at short contact times has been proposed as an efficient means for producing hydrogen from alcohol and hydrocarbons [8–12]. In this process, fuel and oxygen are fed to a noble metal catalyst at high flow rates. The catalyst is initially heated to ignite the reaction; reaction then proceeds autothermally, where the heat from surface oxidation reactions allows further reaction to occur. Running CPO in this fashion offers several advantages. A high production rate of hydrogen is achieved from a small catalyst bed. In addition, hydrogen can be produced almost on demand. Finally, there are no additional heating requirements.

While CPO appears attractive for portable power generation applications, there may be trade-offs for using it. For example, if no water is added to the feed stream of CPO, more carbon monoxide is formed compared to other reforming processes. This will require more intense downstream processing to clean the hydrogen for use by the PEMFC. This paper evaluates the use of CPO in an integrated system for generation of high-purity hydrogen for a PEMFC from a military logistic fuel, JP-8. A fuel processing system using CPO as the first processing step is simulated to understand the trade-offs involved in using CPO. The effects of water flow rate, CPO reactor temperature, carbon to oxygen ratio in the CPO reactor, temperature of preferential oxidation, oxygen to carbon ratio in the preferential oxidation reactor, and temperature for the water-gas shift reaction

* Corresponding author. Tel.: +1 785 532 4315; fax: +1 785 532 7372.
E-mail addresses: hohn@ksu.edu (K.L. Hohn), terry.dubois@us.army.mil (T. DuBois).

0378-7753/$ – see front matter © 2008 Elsevier B.V. All rights reserved.
doi:10.1016/j.jpowsour.2008.04.029

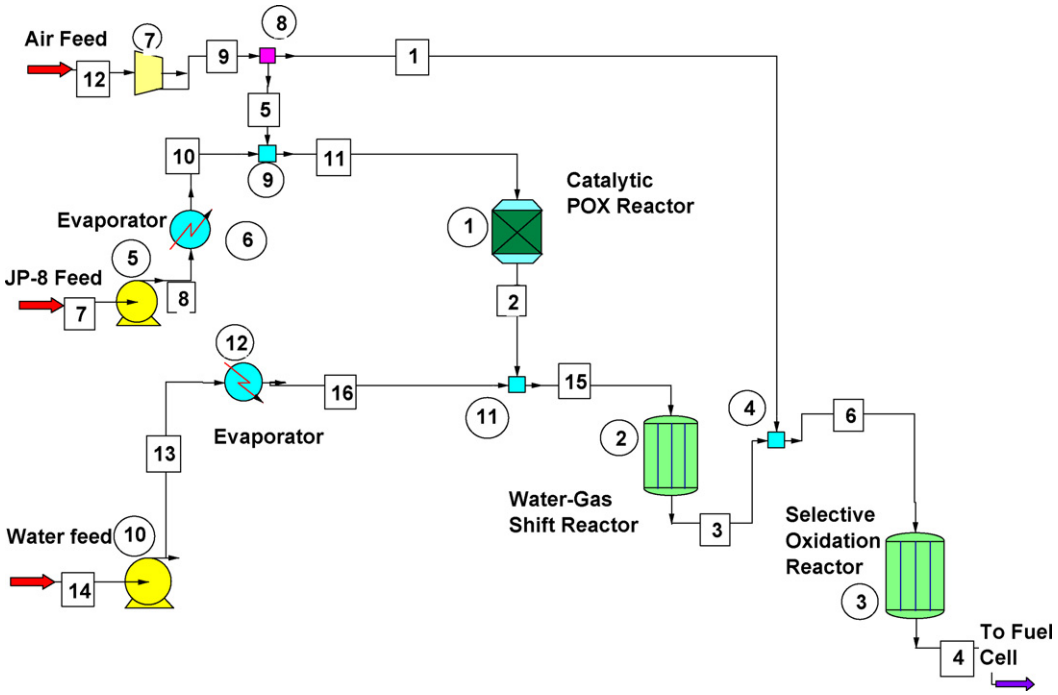

Fig. 1. Flowsheet for JP-8 reforming process.

are evaluated. The possibility of recycling water from the fuel cell for use in fuel processing was evaluated. Finally, heat integration options were explored.

2. Simulation methods

A number of previous studies have simulated fuel processing systems to convert alcohols and hydrocarbons to hydrogen to power a fuel cell [13–16]. Of these simulations, only the work by Ahmed and Krumpelt looks at the potential of CPO for fuel reforming [14]. That work uses stoichiometry and thermodynamics to compare different fuel processing methods (autothermal reforming, steam reforming and catalytic partial oxidation); it does not model the individual fuel processing steps in detail nor does it look at the interplay between those steps. This study focuses on CPO, and in particular how the choice to use CPO as the first step in fuel reforming affects the downstream processing steps. The chemical process simulator, ChemCad, was used to model fuel processing of JP-8 to fuel cell-grade hydrogen.

2.1. Process flowsheet and design basis

Fig. 1 shows the base case process flowsheet for the fuel processing system modeled in this work. In this process, the fuel (JP-8) is vaporized and mixed with air. This combined feed is fed to the catalytic partial oxidation reactor, where the fuel is converted to a stream primarily comprised of syngas (CO and H_2) with some CO_2 and H_2O. The products of the catalytic partial oxidation reactor are mixed with steam, cooled, and fed to a reactor in which the water-gas shift reaction is run. This reactor removes CO from the process stream while producing additional H_2. The third reactor oxidizes the remaining CO to CO_2 to reach a CO concentration of 10 ppm, which would be suitable for a PEMFC.

To simulate JP-8, a mixture of hydrocarbons was assumed. The JP-8 surrogate mixture reported by Sarofim et al. was used [17]. This mixture is composed, by volume, of 10% isooctane, 20% methylcyclohexane, 15% *m*-xylene, 30% *n*-dodecane, 5% tetralin, and 20% *n*-tetradecane, and was developed to closely match the distillation curve and sooting propensity of JP-8. This mixture has a molecular weight of 133.048, and an H/C ratio of 1.91, and can be approximated as $C_{9.57}H_{18.27}$. JP-8 was assumed to be sulfur-free, since sulfur would poison the catalytic partial oxidation reactor. An upstream sulfur-removal process would be needed to achieve the simulated feed, but this process was not modeled in this work.

A primary design variable was the carbon to oxygen (C/O) ratio fed to the CPO reactor. This is defined as the ratio of carbon atoms to oxygen atoms in the feed.

The process was designed to supply a PEM fuel cell with sufficient hydrogen so that it can produce 1 kW of energy. For this power requirement, a H_2 flow rate of ~12–13 standard liters per minute (SLPM) to the fuel cell was required and was the basis for design. This corresponded to a hydrogen molar flow rate of ~0.033 kmol h^{-1}. The primary design constraint was to produce this flow rate of H_2 with less than 10 ppm CO. The amount of water in the feed to the PEMFC was not a consideration. To achieve the specified H_2 flow rate and purity, the size of the reactors and the water flow rate were changed.

2.2. Hydrogen yield and process efficiency

The hydrogen yield was calculated from the ratio of hydrogen produced by the process to the total amount of hydrogen fed to the process, both in JP-8 and as water. The equation used is

$$Y_{H_2} = \frac{F_{H_2}}{F_{H_2Oo} + F_{JP\text{-}8o}} \quad (1)$$

where Y_{H_2} is the yield of H_2, F_{H_2} is the molar flow rate of H_2 at the exit of the process, F_{H_2Oo} is the molar flow rate of H_2O into the process, and $F_{JP\text{-}8o}$ is the molar flow rate of H_2 contained in JP-8 that is fed the process.

The fuel processor efficiency was calculated to compare different process conditions. The efficiency was calculated from the ratio of the lower heating value of the hydrogen produced by the process to the lower heating value of the JP-8 fuel fed to the system.

2.3. Reactors and reaction kinetics

The reactor design and integration of reactors to achieve the required hydrogen flow rate and purity were the primary considerations in this work. The CPO reactor was difficult to model, since experimental kinetics for CPO of higher hydrocarbons were not available. Instead of using a kinetic model, the reaction was assumed to achieve chemical equilibrium. The Gibbs reactor unit operation in ChemCad was used, which minimizes the Gibbs-free energy in order to calculate outlet composition from a given inlet composition and reactor temperature.

The validity of assuming chemical equilibrium was checked by comparing the results of the Gibbs reactor for hexadecane and decane partial oxidation (C/O ratio = 0.6 for hexadecane and C/O ratio = 0.8 for decane) at 970 and 790 °C, respectively, with the experimental results reported from the Schmidt laboratory [18] for the same conditions over a Rh-coated monolith. For both the equilibrium calculation and the experimental results, oxygen was completely converted. Equilibrium calculations predicted essentially complete conversion of the fuels, while the experimental results predicted 95% conversion for decane and ~99% conversion of hexadecane. The equilibrium calculations overpredicted selectivities to H_2 and CO for both fuels while underpredicting selectivities of H_2O and CO_2. This difference is less when hexadecane was the fuel, possibly because the higher temperature allowed reaction to get closer to equilibrium. The equilibrium model predicted a few hundred ppm methane, while experimentally methane was not detected. The major difference between the equilibrium model and the experimental data was that experimentally, the selectivity to olefins (defined as the atoms of carbon present in olefin products divided by the total number of carbon atoms present in all products) was ~5% for either fuel, while the equilibrium calculations predicted no olefin formation.

Although there are differences between the experimental data and the equilibrium predictions, the assumption of chemical equilibrium in the catalytic partial oxidation reactor is not a bad one. This assumption gets worse as the carbon to oxygen ratio gets larger because more olefins are formed experimentally (as much as 80% at high carbon to oxygen ratios), so the simulation was limited to fuel to oxygen ratios of 0.7 for the base case simulations.

The temperature for the CPO reactor was assumed to be the value reported by Krummenacher et al. for catalytic partial oxidation of hexadecane (1273 K for a C/O ratio of 0.7 and a total flow rate (hexadecane, oxygen, and nitrogen) of 2 SLPM) [18]. Pressure drop was not considered. The catalyst was assumed to be a Rh/Al_2O_3 monolith. The reactor volume was found by scaling up the reactor reported in the Krummenacher paper, maintaining the same residence time.

The water-gas shift (WGS) reactor in the model employed a commercial $Cu/ZnO/Al_2O_3$ catalyst. The catalyst bulk density was assumed to be 1.2 g cm^{-3}. Reaction kinetics reported by Choi and Stenger were used [19]. The empirical rate law they derived was of the form:

$$r_{CO} = 2.96 \times 10^5 \exp\left(\frac{-47,400}{RT}\right)\left(P_{CO}P_{H_2O} - \frac{P_{H_2}P_{CO_2}}{K_{eq}}\right) \quad (2)$$

where r_{CO} was the rate of reaction of CO in moles (g cat h)$^{-1}$, R is the gas constant in J (mol K)$^{-1}$, T is the temperature in K, and K_{eq} is the water-gas shift reaction equilibrium constant. All pressures were in atm.

The equilibrium constant was related to T (in K) by the following equation [20]:

$$K_{eq} = \exp\left(\frac{4577.8}{T} - 4.33\right) \quad (3)$$

The WGS reactor was generally assumed to be isothermal at 200 °C. A few simulations were run at different temperatures to determine the effects of temperature on the WGS reactor.

For the preferential oxidation (PROX) reactor, the catalyst was assumed to be a commercial Pt–Fe/γ-alumina catalyst. Catalyst bulk density was assumed to be 1.2 g cm^{-3}. Reaction kinetics reported by Choi and Stenger were used [21]. Their empirically determined kinetics included three separate rate laws to model selective oxidation of CO: CO oxidation, H_2 oxidation, and the water-gas shift reaction. The rate laws used for these three reactions are as follows:

$$-r_1 = 3.528 \times 10^2 \exp\left(\frac{-33,092}{RT}\right) P_{O_2}^{0.5} P_{CO}^{-0.1} \quad (4)$$

$$-r_2 = 2.053 \times 10 \exp\left(\frac{-18,742}{RT}\right) P_{O_2}^{0.5} \quad (5)$$

$$-r_3 = 4.402 \times 10^3 \exp\left(\frac{-34,101}{RT}\right)\left(P_{CO}P_{H_2O} - \frac{P_{CO_2}P_{H_2}}{K_{eq}}\right) \quad (6)$$

where r_1 is the rate of CO oxidation, r_2 is the rate of hydrogen oxidation, and r_3 is the water-gas shift reaction rate. All rates are given in moles (g cat h)$^{-1}$, and activation energies are given in J. Eq. (3) was used to calculate K_{eq} as a function of temperature.

2.4. Heat and mass transfer resistances

Heat and mass transfer resistances, either internal or external to the catalyst, where not explicitly accounted for in any of the three reactors. The CPO reactor likely operates under external mass transfer control due to the extremely high reaction rates at the temperatures of operation. As discussed above, CPO under autothermal conditions approaches equilibrium at a low enough fuel to oxygen ratio (high enough reaction temperature), so mass transfer resistances are implicitly accounted for by using equilibrium to predict the output of the partial oxidation reactor.

The assumption of no transfer limitations in the WGS reactor is a reasonable one if the catalyst size is small enough. Choi and Stenger suggest that the effectiveness factor for a commercial Cu/ZnO catalyst is greater than 0.95 when the catalyst is less than 2 mm [19], so an assumption of no internal mass transfer limitations requires the catalyst to be less than 2 mm.

3. Simulation results and discussion

3.1. Base case

A base case simulation was run with the process conditions shown in Table 1. The results of this simulation are shown in Table 2. Not shown in this table are the minor product flow rates or the nitrogen flow rate. As seen in this table, the CPO reactor produces mostly CO and H_2, with some CO_2 and H_2O. A small amount (1×10^{-7} kmol h^{-1}) of methane was produced in the CPO reactor,

Table 1
Base case conditions for fuel processor simulation

Parameter	Base case value
JP-8 flow rate	0.00349 kmol h^{-1}
Water flow rate (to WGS reactor)	0.02 kmol h^{-1}
C/O ratio (in CPO reactor feed)	0.7
CPO reactor temperature	1223.15 K
WGS reactor temperature	473.15 K
PROX reactor temperature	473.15 K
O_2/CO ratio (in selective oxidation reactor)	1.2
WGS CO outlet composition	1%
Process CO outlet composition	<10 ppm

Table 2
Simulation results for base case conditions

	CPO	WGS	PROX
Product flow rates (kmol h^{-1})			
H_2	0.02171	0.045327	0.044787
CO	0.02542	0.001793	1.31E-6
CO_2	0.007898	0.03152	0.033311
H_2O	0.01014	0.006527	0.00349
Reactor volume (m^3)	0.000043	0.0049	0.000121

but there were virtually no other hydrocarbons exiting the reactor (<10^{-9} kmol h^{-1}). The WGS reactor effectively doubles the flow rate of hydrogen while decreasing the concentration of CO to under 1 mole%. The PROX reactor is necessary to further convert CO to produce a product stream with less than 10 ppm CO. One of the challenges in the PROX reactor is to oxidize CO without oxidizing H_2. As seen in Table 2, there is a small drop in H_2 flow rate in the PROX reactor, as ~1% of the H_2 is converted to water. For the base case simulation, the WGS reactor is by far the largest of the three reactors, with a volume of 0.0049 m^3. This is due to the slow kinetics and to the importance of the WGS reaction in removing CO from the CPO product stream.

3.2. Effect of water molar flow rate

The effect of water flow rate to the WGS reactor was studied, since this parameter will greatly influence the fuel reforming process. The water flow rate was varied from 0 to 0.06 kmol h^{-1}. The base case constraint that the product from the WGS reactor contained 1% CO had to be loosened for water flow rates below 0.02 kmol h^{-1}, since at those flow rates it was not possible to obtain 1% CO. For those conditions, the volume of the WGS reactor was set to give a product composition with the same ratio of products to reactants (i.e. $CO_2 \times H_2/(CO \times H_2O)$ was a constant). All other base case parameters were the same as given in Table 1.

Fig. 2 shows the volumes of the WGS reactor and the PROX reactor for different water flow rates. The WGS reactor has a much larger volume than the PROX reactor by at least a factor of ten for all simulations. Water flow rate has a large effect on the required WGS and PROX reactor volumes. For flow rates below 0.02 kmol h^{-1}, the WGS reactor volume increases while PROX reactor volume decreases as the water flow rate increases. This is because of the constraint at those conditions that the ratio of products to reactants in the WGS reactor exit be the same: more water means that there must be less CO in order for the ratio to be constant. This, in turn, means a higher conversion of CO, which also means that the PROX reactor must oxidize less CO, resulting in a smaller PROX reactor. It should

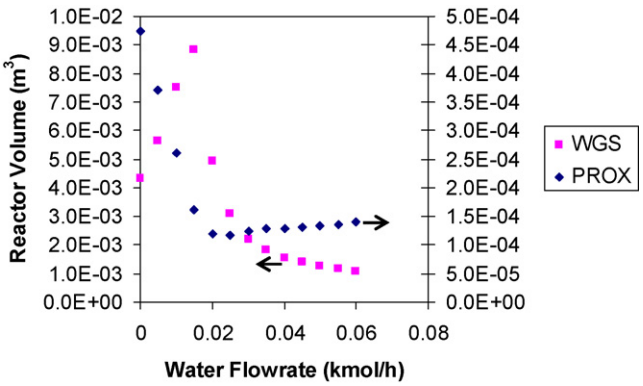

Fig. 2. Reactor volumes for different water flow rates.

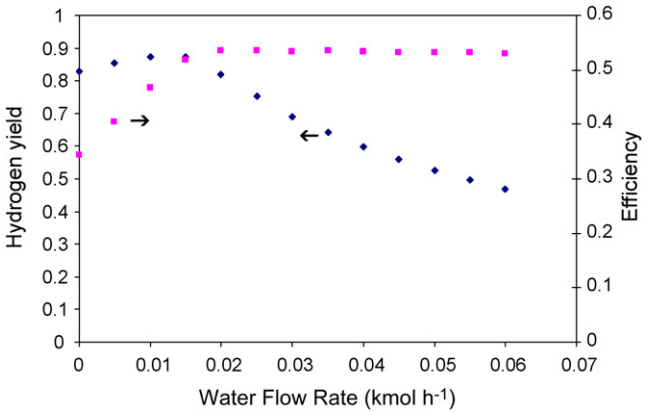

Fig. 3. Hydrogen yield and fuel reformer efficiency as functions of water flow rate.

be noted that using a different constraint would result in a different trend. For example, keeping the hydrogen flow rate exiting the WGS reactor constant would result in lower WGS reactor volumes for increased water flow rates. However, lower water flow rates have limitations on how much hydrogen they can produce because there is insufficient water available to react with CO in the water-gas shift reaction to produce hydrogen in addition to that produced in the CPO reactor.

For 0.02 kmol h^{-1} and greater water flow rates, the constraint of 1% CO at the exit of the WGS reactor can be met. For those flow rates, WGS reactor volume decreases as water flow rate increases due to the increased reaction rate with higher water partial pressure. In addition, the extra water dilutes the CO, so a smaller conversion is needed to achieve the constraint of 1% CO in the WGS reactor exhaust. The PROX reactor volume increases a little with increasing water flow rate because of the slightly higher CO in the WGS reactor exhaust.

Fig. 3 depicts the hydrogen yield and the process efficiency. The hydrogen yield initially increases up to a water flow rate of 0.015 kmol h^{-1}. This increase is due to the increased ability of the WGS reactor to produce hydrogen. At these water flow rates, the WGS reactor is limited by the amount of water: essentially all of the water is converted to hydrogen. At flow rates above 0.015 kmol h^{-1}, the hydrogen yield decreases as the water flow rate increases. This decrease is due to the additional water fed to the WGS reactor that is not converted to hydrogen. If we do not consider the unconverted water into the H_2 yield calculation, hydrogen yield increases up to a flow rate of 0.02 kmol h^{-1}, after which it is relatively constant. The PROX reactor, which converts H_2 to water in a non-selective reaction pathway, has only a slight effect on hydrogen yield, generally decreasing the H_2 yield by only a percent or less.

The process efficiency increases dramatically with water flow rate up to a flow rate of 0.02 kmol h^{-1}, after which it is roughly constant at ~0.53. The process efficiency initially increases with water flow rate because additional hydrogen is produced from the extra water, but then is steady since no additional hydrogen is produced. It should be noted that the definition of process efficiency used only considered the energy content of the hydrogen produced. Energy inputs (for example, the enthalpy needed to vaporize water) was not considered. The process energy balance will be discussed in more detail later in this paper.

3.3. Effect of temperature on WGS reactor

As noted in Section 3.2, the amount of water fed to the WGS reactor has a significant impact on that reactor's performance. Temperature could also impact the performance of the WGS reactor.

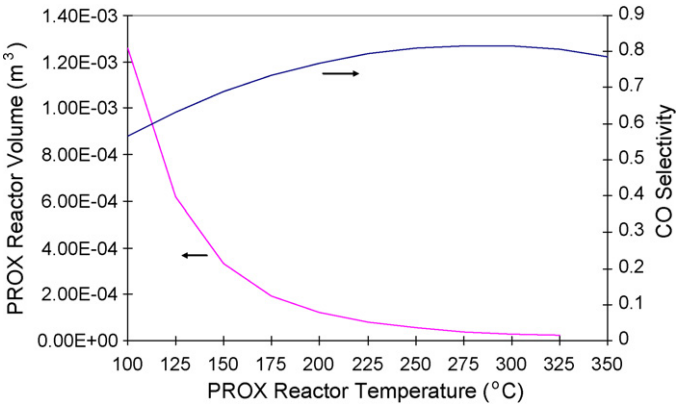

Fig. 4. Effect of reaction temperature on preferential oxidation reactor.

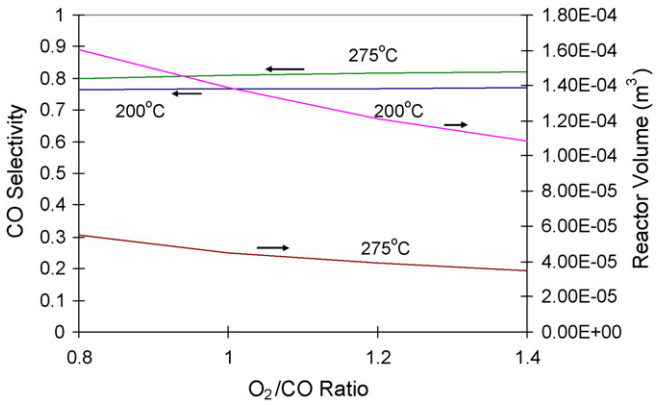

Fig. 5. Effect of O_2/CO ratio on performance of preferential oxidation reactor.

Simulations were run at base case conditions while the temperature of the WGS reactor was varied between 150 and 250 °C. As expected, increasing temperature decreased the reactor volume necessary to reduce the concentration of CO to less than 1%: the required volume was 0.0166 m^3 for a temperature of 150 °C, while it was only 0.00456 m^3 for a temperature of 225 °C. However, when temperature was increased to 250 °C, it was not possible to reduce the CO concentration to the desired level because of equilibrium limitations. This is due to the less favorable equilibrium for WGS at higher temperatures: the equilibrium constant falls from 657.5 at 150 °C to 83.1 at 250 °C. This analysis shows that a balance must be found between more favorable kinetics at high temperatures and more favorable thermodynamics (reaction equilibrium) at low temperatures. A temperature of 200–225 °C appears to be the optimal temperature.

3.4. PROX reactor

The performance of the PROX reactor for different reaction temperatures, O_2/CO ratios, and water inlet flow rates was studied. Reaction temperature was varied from 100 to 350 °C and the O_2/CO ratio was varied from 0.8 to 1.4. The water flow rate was varied as described in Section 3.2. The impact of these changes on CO selectivity (defined as moles of CO converted divided by twice the moles of oxygen converted) and reactor volume necessary to produce a product with less than 10 ppm of CO was studied.

Fig. 4 shows how PROX reaction temperature affects CO selectivity and reactor volume for an O_2/CO ratio of 1.2 and using all base case values. As seen in this figure, reactor volume progressively decreases as reaction temperature increases, reflecting the increased reaction rate as temperature is increased. The CO selectivity increases with reaction temperature up to a temperature of 275 °C, above which it decreases. CO selectivity initially increases with reaction temperature because of the higher activation energy for CO oxidation than for H_2 oxidation. The decrease at high temperatures is due to the inclusion of the water-gas shift reaction [20]. At high temperatures, the reverse water-gas shift reaction begins to be favored, which lowers the CO selectivity by converting CO_2 and H_2 to CO and H_2O. It should be noted that the kinetic model we are using was only validated for temperatures up to 300 °C, so the results above 300 °C may not be completely reliable. We have included these points to determine whether the slight decrease in CO selectivity noted from 275 to 300 °C could be expected to continue, and they show that is does. These results suggest that higher temperatures are optimal for the given inlet composition, with a temperature of 275 °C being the optimal temperature.

The O_2/CO ratio has much less impact on the performance of the PROX reactor when compared to the reaction temperature, as shown in Fig. 5. The CO selectivity increases monotonically with increasing O_2/CO ratio, while the reactor volume required to achieve a CO conversion of >99.9% (outlet CO composition of <10 ppm) decreases. This trend is seen for either 200 or 275 °C. Increased oxygen in the system increases the reaction rates of both CO and H_2 oxidation, leading to the lower reactor volumes to achieve 99.9% conversion. CO selectivity changes little with O_2/CO ratio because the dependences of CO and H_2 oxidation on oxygen are the same (one-half power). It is best to operate the PROX reactor with a high O_2/CO ratio in order to give a lower reactor volume and a (slightly) higher CO selectivity.

Water could have an impact on the PROX reactor performance because of the inclusion of the water-gas shift reaction in the kinetic model. The water flow rate was changed by changing the total molar flow rate of water into the fuel reforming system, as discussed in Section 3.2. Fig. 2 shows that the PROX reactor volume increases slightly with increasing water flow rate. This is not due to the performance of the PROX reactor, but rather is due to the higher concentration of CO in the feed to the PROX reactor. When simulations were run with varying water inlet composition, but constant CO composition, the PROX reactor volume decreased with increasing water molar flow rate because the water-gas shift reaction is able to convert some of the CO to CO_2. The CO selectivity increased with increasing water molar flow rate, going from 0.768 at a water molar flow rate of 0.02 kmol h^{-1} to 0.844 at a water molar flow rate of 0.06 kmol h^{-1}. Again, this trend indicates the influence of the water-gas shift reaction on the PROX reactor performance. These simulations suggest that that the optimal operating conditions for the PROX reactor are with a larger water flow rate.

3.5. Effect of catalytic partial oxidation temperature

The temperature of the catalytic partial oxidation reactor cannot be easily varied, but is instead determined by the reactant conversion, product selectivity, and the heat losses from the reactor. This temperature has not been measured for JP-8 or its simulant. For the base case solution, a temperature equal to that reported for hexadecane catalytic partial oxidation at a C/O ratio of 0.7 was used.

The effects of changing this temperature on the fuel reformer performance were studied. The temperature was varied between 1173 and 1323 K. This temperature range was chosen because it is similar to the values measured in experimental work on hexadecane catalytic partial oxidation [18]. As noted above, the CPO

Table 3
Simulation results when CPO reaction temperature was varied

	1173 K	1223 K	1273 K	1323 K
CPO product flow rate (kmol h^{-1})				
H_2	0.0222	0.0217	0.0213	0.0210
CH_4	8.01×10^{-7}	2.84×10^{-7}	1.06×10^{-7}	4.48×10^{-8}
CO	0.0250	0.0254	0.0258	0.0262
CO_2	0.0084	0.0079	0.0075	0.0071
H_2O	0.0097	0.0101	0.0105	0.0109
WGS volume (m^3)	0.0048	0.0049	0.0049	0.0049
PROX volume (m^3)	1.17×10^{-4}	1.12×10^{-4}	1.12×10^{-4}	1.12×10^{-4}
H_2 yield	0.818	0.818	0.818	0.818
Process efficiency (%)	0.534	0.535	0.534	0.534

temperature cannot be independently varied due to the autothermal nature of the reaction; however, adding diluent to the feed, preheating the feed, and providing external heating/cooling to the reactor can change the temperature, and would allow the temperature range simulated. Table 3 shows the product composition exiting the CPO reactor at four different CPO reaction temperatures. It also shows the hydrogen yield, the process energy efficiency, and the volume of the WGS and PROX reactors at base case conditions except for CPO reaction temperature.

As seen in this table, as the temperature increases, the molar flow rates of H_2 and CO_2 decrease and the molar flow rats of H_2O and CO increase. Lower temperatures result in more methane produced: the methane molar flow rate increases by more than an order of magnitude as temperature is decreased from 1323 to 1173 K, although it is still very small. Temperature affects the CPO product composition in the simulation by shifting reaction equilibrium to different products. Despite the differences in product composition exiting the CPO reactor, the WGS and PROX reactor sizes required to meet the desired product specifications are virtually the same for all temperatures. In addition, the H_2 yield and the process efficiency do not change with CPO reaction temperature.

It is somewhat surprising that changes in the product composition following the CPO reactor have little influence on the downstream processing, either in the volume requirements or the process efficiency. This can be explained in two ways. First of all, the changes in CPO product composition are small: the change in H_2 and CO molar flows is only ~5% going from the lowest to the highest temperature. Secondly, the increased CO molar flow rate means that the WGS reactor has more CO to convert, but the reaction kinetics in the WGS reactor are faster due to higher CO and H_2O partial pressures. This results in virtually the same WGS reactor volume for all CPO reaction temperatures.

These results suggest that CPO reaction temperature is not an important parameter in the temperature range investigated. This does not mean that CPO reaction temperature is always unimportant; on the contrary, CPO temperature is likely crucial to the success of using CPO for a fuel reformer. Our assumption is that reaction equilibrium is achieved in the CPO reactor, but this will only be achieved or approached at the highest reaction temperatures. Lower temperatures result in more formation of olefins and methane, which will not be substantially converted in the rest of the fuel reformer and represent a loss of hydrogen (loss of process efficiency). In addition, all of the fuel will not be converted at lower temperatures, which also results in a loss of efficiency. Running the CPO reactor at higher temperatures, therefore, appears to be the best option since it will ensure production of nearly all partial and complete oxidation products, even though the selectivity to H_2 and CO_2 may suffer at higher temperatures.

3.6. Water recycle

As shown above, water addition is critical to achieving the desired H_2 production rate and purity. For practical application, it would be desirable if additional water did not need to be carried in order to operate the fuel reforming process. This could be achieved if the fuel cell produced enough water to supply the water for the water-gas shift reaction. Simulations were run to determine if this was the case.

To simulate water recycle, the base case process flow sheet was modified so that the products of the fuel processor were fed to a reactor (the fuel cell) and reacted with oxygen. Following the reactor, the products were condensed at 298 K and the condensed phase was pumped to an evaporator and subsequently to the WGS reactor. It was assumed that 70% of the hydrogen reacted with oxygen in the fuel cell to form water.

The fuel processor with water recycle was simulated with a WGS reactor volume of 0.0026 m^3 and a PROX reactor volume of 1.21×10^{-4} m^3. All other conditions were kept the same as for the base case simulation, except that the flow of water to the WGS reactor was not varied independently since it came from the recycle stream. In this simulation, 0.0448 kmol h^{-1} of hydrogen was produced with a CO flow rate of 7.317×10^{-7} kmol h^{-1}. This hydrogen production rate resulted in a water recycle rate of 0.027 kmol h^{-1}, with 0.0043 kmol h^{-1} water exiting in the non-condensed stream. The fuel reforming process efficiency when water recycle was used was 0.535, similar to process efficiencies without water recycle. Water recycling appears feasible to provide all of the necessary water for the water-gas shift reaction.

3.7. Heat integration

Applying CPO for fuel reforming provides several opportunities for heat integration due to the high exothermicity of CPO. Fig. 6 shows the enthalpy changes in most of the unit operations in the fuel reformer process for different water molar flow rates. Not shown are enthalpy changes in pumps, which are negligible compared to other unit operations, or the enthalpy change for JP-8 evaporation, which is constant at a value of 0.304684 MJ h^{-1}.

As seen in Fig. 6, the total enthalpy change for the fuel reformer is negative for all flow rates. The CPO reactor and the heat exchanger, which lowers the temperature of the stream exiting the CPO reactor to the temperature of the WGS reactor, release most of the energy. The PROX reactor releases a lot of energy at low water flow rates (−4.67 MJ h^{-1} at 0 kmol h^{-1}), when PROX is needed to achieve

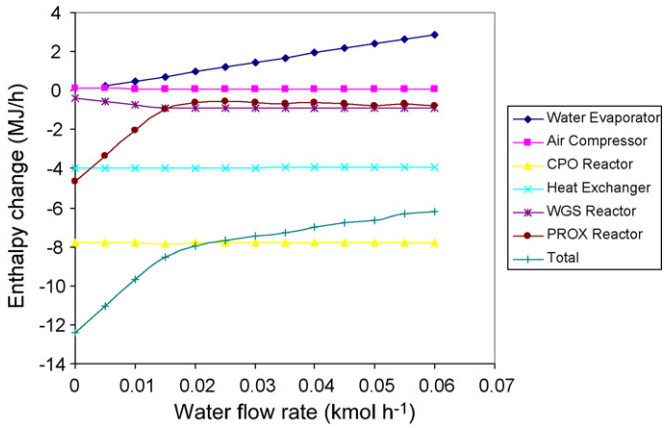

Fig. 6. Enthalpy changes in important unit operations and for the entire fuel processor.

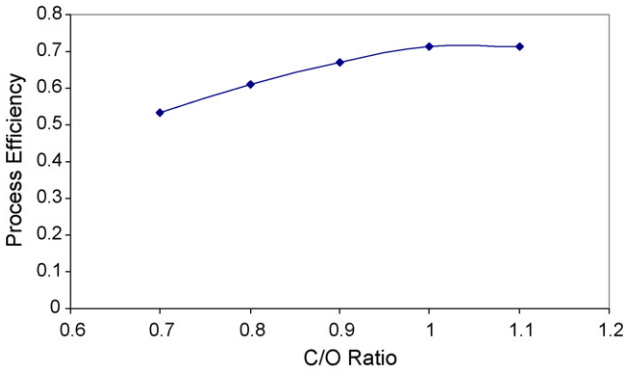

Fig. 7. Fuel reformer efficiency for different carbon to oxygen ratios in CPO reactor.

10 ppm CO. However, it releases less energy as the water flow rate is increased because the water-gas shift reactor is capable of removing more of the CO and the PROX reactor is much smaller. The fuel reforming process releases less energy as the water flow rate is increased because of the higher energy inputs required to vaporize water. Water vaporization is the largest energy sink in the process. The enthalpy changes in the CPO reactor, WGS reactor, and the heat exchanger are relatively constant with water flow rate.

These results show that the energy inputs required for vaporization of water and JP-8 can easily be achieved using waste heat from the CPO reaction. However, the results also show why the process efficiency is not higher: much of the energy of JP-8 is going to produce heat, not hydrogen.

3.8. Carbon to oxygen ratio of feed to CPO reactor

The process efficiencies for the base case simulations are not particularly high. This is due, in large part, to the large amount of oxygen fed to the CPO reactor that results in complete oxidation products. Clearly, one way to address this issue is to change the carbon to oxygen ratio in the feed to the CPO reactor. The reforming system was simulated with different carbon to oxygen ratios fed to the CPO reactor. To accomplish this, the JP-8 flow rate was held constant, while the flow rate of air to the CPO reactor was changed. The CPO reactor temperature was held constant at 1223.15 K and the water flow rate was 0.04 kmol h^{-1}.

As the carbon to oxygen ratio was increased, the selectivities of hydrogen and carbon monoxide increased. This meant that larger WGS reactors were required to convert the additional CO to CO_2; however, it also led to higher process efficiencies. Fig. 7 shows the process efficiency for different carbon to oxygen ratios. As seen in this figure, the process efficiency increases significantly as the carbon to oxygen ratio increases from 0.7 to 1, but then is level upon going from 1 to 1.1. The leveling off of process efficiency results from the nearly identical hydrogen selectivities in the CPO reactor at carbon to oxygen ratios of 1 and 1.1.

It should be noted that much of the process efficiency comes from the processing steps after the CPO. Calculating the process efficiency using the products of CPO, the efficiency is roughly half of the ultimate process efficiency. For example, at a C/O ratio of 0.7, the efficiency of the CPO reactor alone is 0.259, while it is 0.356 at a C/O ratio of 1.1. This is because the CPO reactor is effective at reacting JP-8, but only is responsible for roughly half of the ultimate hydrogen formed in the process.

While the simulations predict increased process efficiency with increasing carbon to oxygen ratio, the situation may not be this simple in practice. Experimental results for CPO of hexadecane and decane show that increasing carbon to oxygen ratio results in high selectivity to olefins [18], partly because of the lower autothermal reaction temperatures at those conditions. Therefore, the simulations over-predict the process efficiency at higher carbon to oxygen ratios because the simulated CPO reactor does not predict extensive olefin formation. To account for this, a simulation was performed at a carbon to oxygen ratio of one where the product stream exiting the CPO reactor was estimated from the experimental data reported by Krunemacher et al. This stream was then fed to the WGS and PROX reactors. The process efficiency for this simulation was found to be only 0.53, as opposed to the efficiency of 0.71 predicted for the same carbon to oxygen ratio when the CPO reactor was assumed to reach equilibrium. The formation of olefins, therefore, lessened the process efficiency by 0.18.

These results suggest that CPO could provide process efficiencies over 70% if olefin production is minimized. This could be achieved by using different catalyst formulations. In addition, addition of steam to the CPO feed could decrease formation of olefins. It is recognized, in general, that addition of steam to the CPO feed may be advantageous for increased hydrogen yield and decreased production of carbon and other side products; however, steam addition was not considered in this paper

Another factor when considering C/O ratio is the potential for coke formation. The equilibrium model used to simulate the CPO reactor assumed coke-free operation, and this is consistent with the experimental results obtained by Krummenacher et al. [18]. However, there is potential for carbon formation if there is insufficient oxygen. Shekhawat et al. reported that carbon-free operation will be achieved in CPO for O/C ratios above 1.1 (C/O ratio less than 0.9) [6]. Again, this suggests that while the higher C/O ratios appear to give higher overall process efficiency, these ratios may not be desirable because of other considerations.

4. Conclusions

Simulations show that using catalytic partial oxidation as the first step in reforming of JP-8 to hydrogen is feasible as long as sufficient water is fed to a water-gas shift reactor. The base case simulation showed that 0.0448 kmol h^{-1} H_2 could be produced from JP-8 with a water flow rate of 0.02 kmol h^{-1}, a catalytic partial oxidation reactor of 0.000043 m^3, a water-gas shift reactor of 0.0049 m^3, and a preferential oxidation reactor of 0.000121 m^3. The water flow rate is critical to production of a CO-free H_2 stream: flow rates below 0.02 kmol h^{-1} did not produce the desired hydrogen flow rate, while large water flow rates led to smaller water-gas shift reactors and slightly larger preferential oxidation reactors. Recycling water from the exhaust of the fuel cell to the water-gas shift reactor could allow the process to operate without an external supply of water. In addition, heat integration allows the process to operate without any external source of heat, since catalytic partial oxidation provides sufficient energy to vaporize water and JP-8. A process efficiency, defined as the ratio of the lower heating value of hydrogen to that of JP-8, of around 53% is possible using catalytic partial oxidation as the first step in JP-8 reforming. Higher efficiencies are possible (up to 71%) when higher C/O ratios are used, provided that olefin production can be minimized in the catalytic partial oxidation reactor.

References

[1] C.S. Song, Catal. Today 77 (2002) 17–49.
[2] F. Joensen, J.R. Rostrup-Nielsen, J. Power Sources 105 (2002) 195–201.
[3] M. Krumpelt, T.R. Krause, J.D. Carter, J.P. Kopasz, S. Ahmed, Catal. Today 77 (2002) 3–16.
[4] Y.T. Seo, D.J. Seo, J.H. Jeong, W.L. Yoon, J. Power Sources 163 (2006) 119–124.
[5] A. Lindermeir, S. Kah, S. Kavuruc, M. Muhlner, Appl. Catal. B Environ. 70 (2007) 488–497.

[6] D. Shekhawat, D. Gardner, J.J. Spivey, Catalysis 19 (2006) 184–254.
[7] D.L. Trimm, Z.I. Onsan, Catal. Rev. 43 (2001) 31–84.
[8] G.A. DeLuga, J.R. Salge, L.D. Schmidt, X.E. Verykios, Science 303 (2004) 993–997.
[9] B.E. Traxel, K.L. Hohn, Appl. Catal. A: Gen. 244 (2003) 129–140.
[10] D.A. Hickman, L.D. Schmidt, Science 259 (1993) 343–346.
[11] R. Subramanian, G.J. Panuccio, J.J. Krummenacher, I.C. Lee, L.D. Schmidt, Chem. Eng. Sci. 59 (2004) 5501–5507.
[12] A. Beretta, P. Forzatti, Chem. Eng. J. 99 (2004) 219–226.
[13] S.K. Kamaruidn, W.R.W. Som, A.M. Mohammad, S. Takriff, M.S. Masder, Chem. Eng. J. 103 (1996) 99–113.
[14] S. Ahmed, M. Krumpelt, Int. J. Hydrogen Energy 26 (2001) 291–301.
[15] E.D. Doss, R. Kumar, R.K. Ahluwalia, M. Krumpelt, J. Power Sources 102 (2001) 1–15.
[16] J.C. Amphlett, R.F. Mann, B.A. Peppley, P.R. Roberge, J.P. Salvado, J. Power Sources 71 (1998) 179–184.
[17] A.F. Sarofim, E.G. Eddings, S. Yan, A. Violi, S. Granata, T. Faravelli, E. Ranzi, in: M. Kamel, M.S. Mansour (Eds.), Proceedings of the Second Mediterranean Combustion Symposium, Sharm El-Sheikh, Egypt, January 6–11, 2002, pp. 961–971.
[18] J.J. Krummenacher, K.N. West, L.D. Schmidt, J. Catal. 215 (2003) 332–343.
[19] Y. Choi, H.G. Stenger, J. Power Sources 124 (2003) 432–439.
[20] J.M. Mo, Chem. Eng. Proc. 58 (1962) 33–36.
[21] Y. Choi, H.G. Stenger, J. Power Sources 129 (2004) 246–254.